

## ENHANCED STRUCTURE, COMPOSITION, AND PROPERTIES OF $\text{CuCr}_{1-x}\text{O}_2$ THIN FILMS

**P. Sateesh<sup>1\*</sup>**

<sup>1</sup>Department of Physics, St. Peter's Engineering College, T.S, 500100, India

**K. Ashalatha<sup>2</sup>**

<sup>2</sup>Department of Physics, CMR College of Engineering and Technology, TS, 501401, India

**A. Mallikarjun<sup>3</sup>**

<sup>3</sup>Department of Physics, CMR College of Engineering and Technology, TS, 501401, India

**Poornima B. Shetty<sup>4</sup>**

<sup>4</sup>Department of Humanities and Sciences, CVR College of Engineering, Vastunagar, Mangalapalli(V), Ibrahimpatnam(M), R.R District, TS, 501510, India.

**Asam Rajesh<sup>5</sup>**

<sup>5</sup>Department of Physics, St. Peter's Engineering College, T.S, 500100, India

**Y. Durga Sravanthi<sup>6</sup>**

<sup>6</sup>Department of Chemistry, St. Peter's Engineering College, T.S, 500100, India

*Corresponding Author:*  
[satheesh.poonam@gmail.com](mailto:satheesh.poonam@gmail.com)

### **Abstract**

$\text{CuCr}_{1-x}\text{O}_2$  thin films was synthesized by a sol-gel technique. In this study structural, optical and electrical properties of  $\text{CuCr}_{1-x}\text{O}_2$  films ( $x = 0, 0.1, 0.15, 0.2, 0.3$ ) which exhibited p-type properties, were investigated. Using Combustion chemistry, films are solution processed at  $150^\circ\text{C}$  which is lower than most recent efforts. Smooth and homogeneous thin films are obtained at the pretreated temperature at  $450^\circ\text{C}$ .  $\text{CuCr}_{1-x}\text{O}_2$  thin films have been annealed at different temperatures (from  $600$  to  $900^\circ\text{C}$ ). The films were characterized by XRD, FE-SEM, FTIR and Hall Effect measurement. The optical band gap as determined from FTIR measurements is observed ranging between  $3.12$  and  $3.2$  eV the lowest resistivity was obtained with annealing at  $800^\circ\text{C}$ ,  $92.85 \Omega \text{ cm}$  respectively. The results exhibited Superior optoelectronic Characteristics with interesting temperature-dependent copper delafossite thin films.

**INTRODUCTION:**  $\text{CuCrO}_2$  films with p-type conductivity are broadly used as critical components used in both light emitting device Mechanism In this contemporary work, we have

adapted CuCrO<sub>2</sub> thin films with different concentration of Cr<sup>3+</sup> (0.05M, 0.1M, 0.15M, and 0.2M, 0.3M) on Glass substrate by simple sol-gel spin coating Method. Different members of the copper delafossite family exhibit both good transparency and p-type electrical conductivity [1-5]. The latter are therefore of great interest in optoelectronics, in particular for developing transparent light-emitting diodes. However, delafossites often require heat treatments at high temperature ( $\geq 600$  °C for CuCrO<sub>2</sub>) in order to achieve sufficient electronic and optical properties from the point of view of technological applications [6-12]. This constraint therefore excludes the use of many usual substrates of polymer type and even ordinary glass [13-17]. However, the techniques of direct writing laser, which make it possible to strongly heat a layer absorbing the wavelength of the laser, while only slightly raising the temperature of a transparent substrate, could make it possible to circumvent this limitation [18-19]. The control of the laser spot on a micron scale would also allow the production of specific patterns, sometimes required by transparent electronics.

## 1. Experimental:

In this exercise specified amount of Cu (CH<sub>3</sub>COO)<sub>2</sub>H<sub>2</sub>O (99%) and Cr(NO<sub>3</sub>)<sub>3</sub>9H<sub>2</sub>O (99%) were fused in 20ml propionic acid. The metallic ion (Cu<sup>2+</sup> and Cr<sup>3+</sup>) concentrations were 0.05M, 0.1M, 0.15M and 0.2M (Cr<sup>3+</sup>). The admixtures were stirred for many hours in order to get a transparent solution. The solution was spin-coated onto Glass substrates at a rate of 8000 r/min, Preheated at 400–550 °C for 30 min in air. Later repeated the above illustrate procedure five times, all the films were finally sintered in a furnace 900°C.

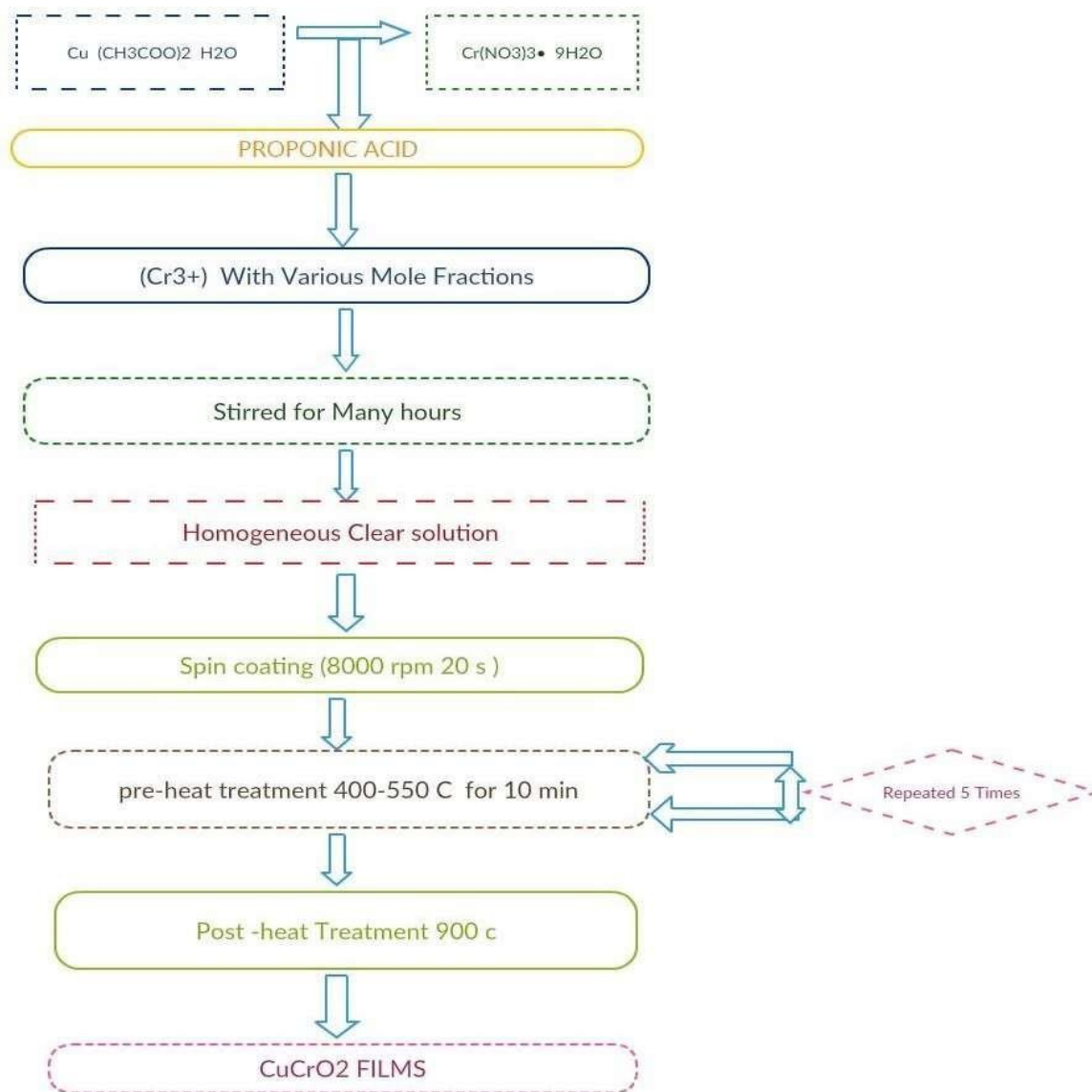


Figure1.1: The Flowchart for the preparation of the  $\text{CuCrO}_2$  thin films by the sol-gel spin-coating method.

. Results and Discussion:

XRD STUDY:

This Shows the XRD results of the  $\text{CuCrO}_2$  films pretreated at varying temperatures (400–900 °C), sintered at 900 °C. From the XRD results, it can be erect that the films pretreated at temperatures of 400–900°C are Composed of single Structured  $\text{CuCrO}_2$  phase, as shown by D in Fig. 1.2 without any detectable undesired phases. Moreover, it can be observed that the peak at  $31.4^\circ$  is especially sharp and have a compelling lower line width than the other signals

Sherrer formula:  $D = K\lambda / \beta \cos\theta$ .

Where  $\lambda$  is the wavelength of  $\text{CuK}\alpha$  radiation (0.154nm),

$k=0.9$  is the shape factor

$\Theta$  is the Bragg angle and

$\beta$  is the experimental full-width at half maximum on the respective diffraction peak

The Crystalline size Calculated by applying the Scherer formula Associated to the peaks at  $31.6^\circ$  and Corresponding to the (003). The Crystalline size also increases from 29nm to 78nm

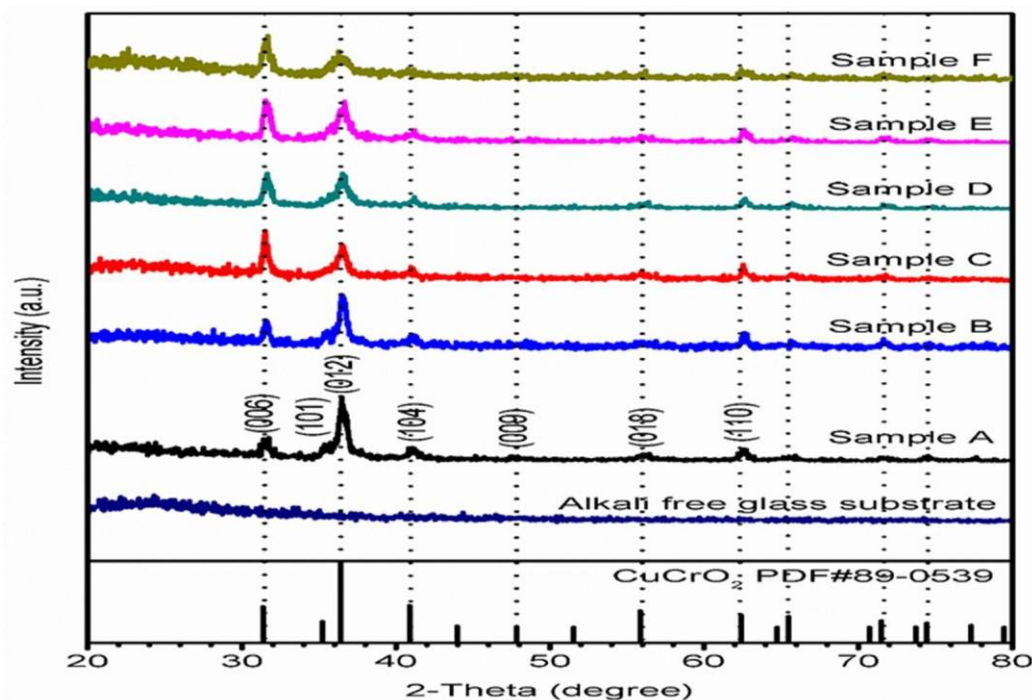


Figure 1.2 shows the XRD patterns of the sol-gel derived films. After sintering at  $600^\circ\text{C}$  in  $\text{N}_2$  atmosphere for 1h phase pure  $\text{CuCr}_{1-x}\text{O}_2$  films (R3M, JCPDS #C89-6744) are obtained above  $700^\circ\text{C}$ ,  $800^\circ\text{C}$  and  $900^\circ\text{C}$  (003), (006) diffraction peaks appeared .

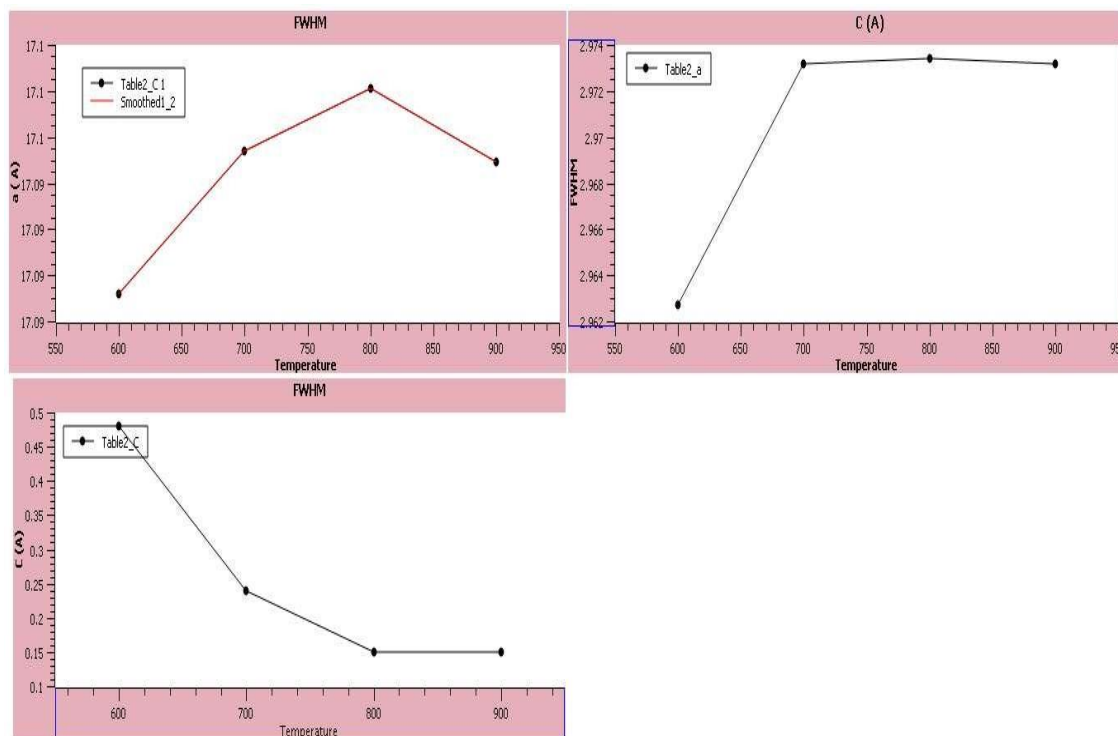


Figure 1.3 Shows the Lattice Parameters (a and c) Through Temperature and FWHM

Figure 1.3 Shows the variations in the FWHM and the crystalline size as a function of annealing temperature obtained by (006) signal at  $31.4^\circ$ . The values of the full width at half Maximum (FWHM) for the (006) diffraction peak were 0.48(600°C), 0.24 (700°C) 0.15 (800°C), and 0.15 (900°C).

Table: 1.1 Lattice parameters a and c of CuCrO<sub>2</sub> films with different annealing temperature

| CuCrO <sub>2</sub> films | 600°C   | 700°C   | 800°C   | 900°C   |
|--------------------------|---------|---------|---------|---------|
| a(Å)                     | 2.9627  | 2.9732  | 2.9734  | 2.9732  |
| c (Å)                    | 17.0892 | 17.0954 | 17.0981 | 17.0949 |

### 3. Morphology and Compositional Analysis

The SEM images of Surfaces of CuCrO<sub>2</sub> Films 0.2M the surfaces of thereare smooth and fine particles. No cracks exist at the surface. As a result, we could assume that the crystallinity of CuCoO<sub>2</sub> retains a structure mostly constituted of nanocrystals smaller than 15 nm in diameter

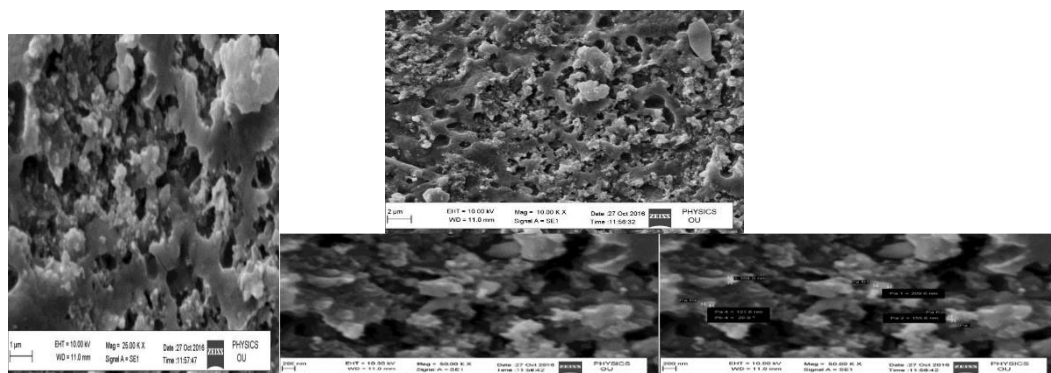
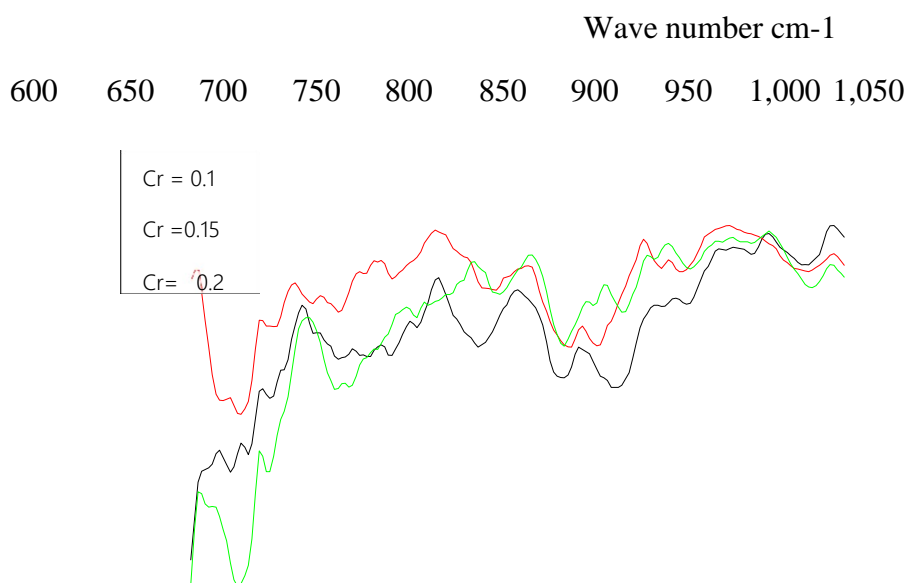


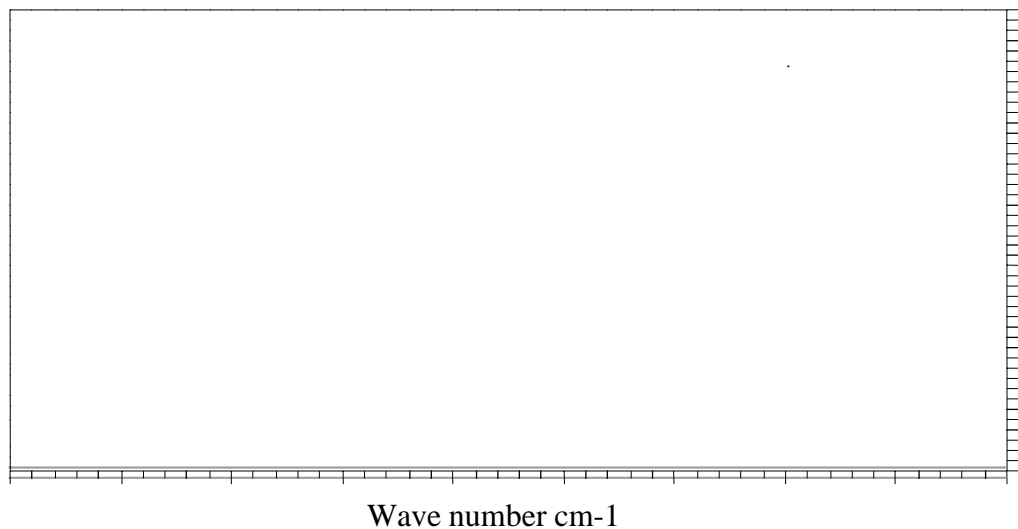
Figure 1.5 SEM IMAGES OF 0.2 M

#### 4. Optical study:

The FT-IR spectrum of the  $\text{CuCrO}_2$  Films is shown in Fig. 1.5 Shows one weak ( $958 \text{ cm}^{-1}$ ) and five strong bands ( $675, 734, 750, 765$  and  $781 \text{ cm}^{-1}$ ) could be assigned to the  $\text{Cr}^{\text{III}}\text{-O}$ , and  $\text{M-O}$  bond stretching frequencies of the  $\text{CuCrO}_2$  Films. The FT-IR spectrum of the  $\text{CuCrO}_2$  films good agreement with Experimental value.

#### FTIR GRAPHS $\text{CuCrO}_2$ FILMS



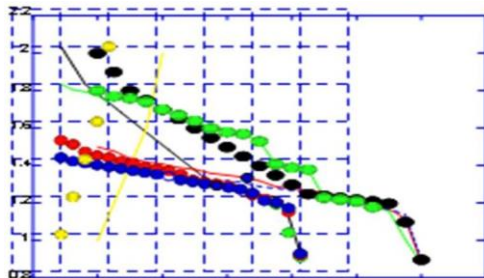


1.6 FTIR SPECTRUM OF  $\text{CuCrO}_2$  FILMS  $\text{Cu} = 0.2 \text{ M}$  AND  $\text{Cr} = 0.1 \text{ M}, 0.15 \text{ M}$  AND  $0.2 \text{ M}$

### 5. Thermo electric Properties and Conductivity

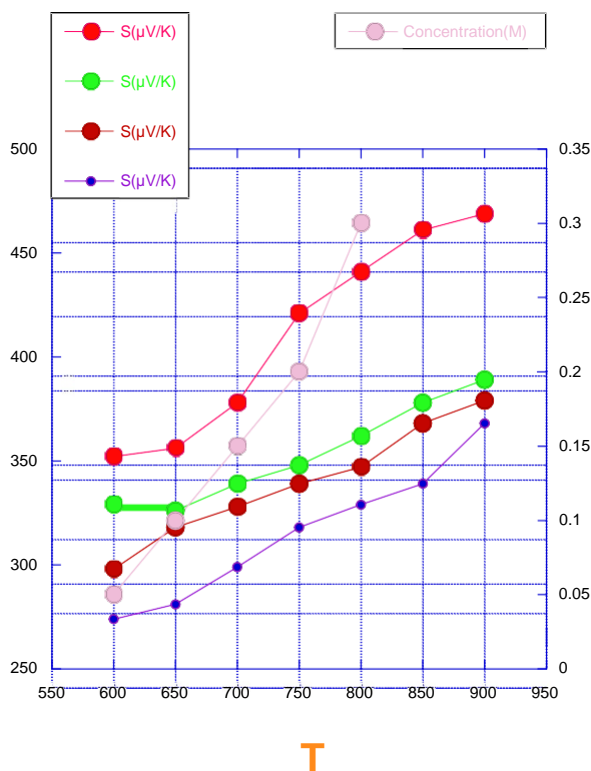
In figure 1.7 we show the electrical transport measurements on the same films annealed at various temperatures  $600\text{-}900^\circ \text{C}$ . As shown in Figure 3a, for all the films the T dependence of resistivity shows a purely semiconducting behavior with  $dU/dT < 0$  as the temperature is increased. Annealing effect on the films is observed as the reduction in the total resistivity probably due to phase conversion of remnant  $\text{CuO}$  and  $\text{CuCr}_2\text{O}_4$  to  $\text{CuCrO}_2$ .<sup>31</sup> The resistivity of the film with maximum proportion of  $\text{CuCrO}_2$  (i.e. film annealed at  $900^\circ \text{C}$ ) matches well with the values reported in literature.

Figure 1.8 shows the T dependence of Seebeck coefficient of the same films. The positive Seebeck values confirm the p-type conductivity of the films. Quantitatively the room temperature Seebeck values do not change much with higher annealing temperatures however show an increasing trend with values  $\sim 300\text{-}325 \pm 10 \text{ PV/K}$ . This is comparable ( $\sim 350 \text{ PV/K}$ ) to the value reported by T. Okuda et al.<sup>18-20</sup> for powder samples of Mg doped  $\text{CuCrO}_2$ . However, much higher ( $\sim 1200 \text{ PV/K}$ ) values have been reported by Benko, Koffyberg<sup>11</sup> and Y. Ono et al.<sup>18</sup> for bulk powdered samples of Ca and Mg doped  $\text{CuCrO}_2$  respectively. This is believed to be related to the large resistivity differences<sup>32</sup> of their materials ( $\sim 100: \text{cm}$ ) to the films we measured ( $\sim 1.0: \text{cm}$ ). It is to be mentioned that the T dependence of resistivity and Seebeck coefficient for all the films show similar character irrespective of their nature and remnant composition.



**Figure 1.7 Temperature Dependent Resistivity with Concentration**

We can use four probe techniques to measure the potential drop between two electrodes when a constant known current flows between other two electrodes and then calculating conductivity using the geometry of electrodes. Delafossite characteristic diffraction peaks were obtained as a function of the thermal treatment. The electrical conductivity was optimized until  $1.6 \text{ S cm}^{-1}$  is good agreement with literature value.



**Figure 1.8 Temperature dependence Seebeck coefficients with Concentration**



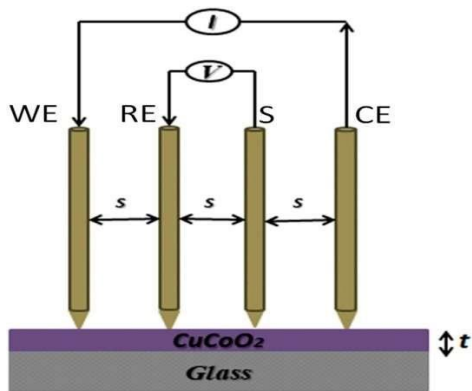
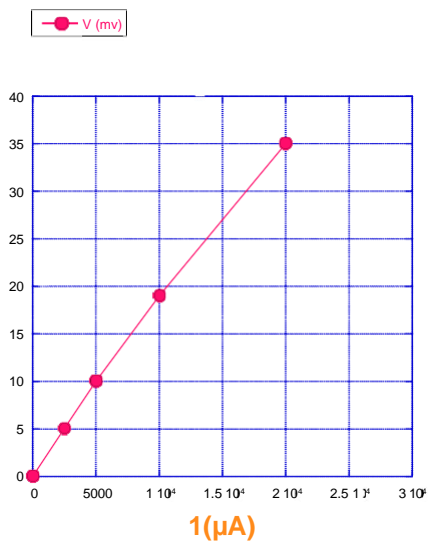


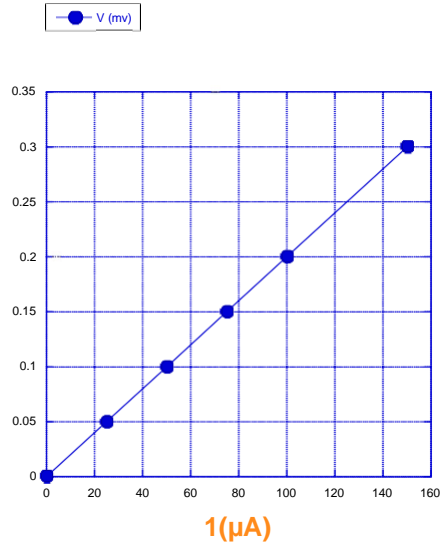
Figure 1.9 Four Probe Point Experiment

The experimental procedure used is the following. The four point probe is attached to a source meter that may supply a certain current. A source meter's current ( $I$ ) flows through the two outer probes, and a voltmeter can measure the voltage ( $V$ ) across the two inner probes. Plotting the voltage measured for each current intensity permit us determine the sheet resistance,  $R_s$ , such as is shown in Figure 2.1, 2.2 and 2.3

2.1:  $\text{CuCrO}_2$  \_ 0.1 M I-V



2.2:  $\text{CuCrO}_2$  \_0.2 M I-V



2.3 CuCrO<sub>2</sub>\_ 0.3 M I-V

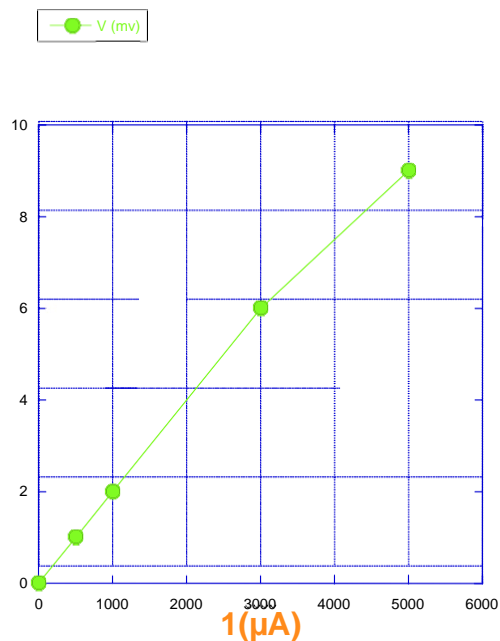


Table 1.2: The electrical properties of the CuCrO<sub>2</sub> thin films determined at annealing temperature

| <i>Samples</i>                 | <i>Sheet Resistivity</i> ( $\square s$ )<br>$\times 10^{-3}$ ( $\Omega.cm$ ) | <i>Sheet resistance</i> ( <i>Rs</i> )<br>( $\Omega$ ) | <i>Sheet Conductivity</i><br>$\times 10^3$ ( $S.cm^{-1}$ ) |
|--------------------------------|--|---|--|
| <b>CuCrO<sub>2</sub>_0.1 M</b> | 0.117 ±0.002   | 8.19±0.05   | 8.9±0.2  |
| <b>CuCrO<sub>2</sub>_0.2 M</b> | 0.108±0.002  | 7.79±0.04   | 9.6±0.2  |
| <b>CuCrO<sub>2</sub>_0.3 M</b> | 0.119±0.002  | 8.17±0.04   | 8.7±0.2  |

5. Conclusions

In this work, we presented the structural, optical and electronic transport properties of CuCrO<sub>2</sub> thin films fabricated through an Sol-gel Method. Though the study was particularly intended to the growth of high-quality CuCrO<sub>2</sub> films the information of the process parameters and growth characteristics may also be useful for the deposition of other members of the CuAO<sub>2</sub> delafossite

family for potential TCO applications. The as-deposited films exhibited smooth homogeneous surfaces but were non-crystalline; annealing at 600-900 °C in Ar then revealed crystalline CuCrO<sub>2</sub> films. With higher annealing temperature optical transmittance of the films improved to greater than 75% in the visible range with the direct bandgap of 3.09 eV. One higher- energy sub-band transition was observed at 3.54 eV. Electrical transport measurements confirm the p- type semiconducting behavior of the films.

## References:

- R. W. Johnson, A. Hultqvist, and S. F. Bent, *Materials Today* 2014, 17 (5), 236.
- V. Miikkulainen, M. Leskelä, M. Ritala, and R. L. Puurunen, *Journal of Applied Physics* 2013. 113, 021301.
- S. Seki, Y. Onose and Y. Tokura, *Phys. Rev. Lett.*, 2008, 101, 067204.
- H. Kawazoe, M. Yasukawa, H. Hyodo, M. Kurita, H. Yanagi, and H. Hosono, *Nature* (London), 1997, 398, 939.
- H. Yanagi, T. Hase, S. Ibuki, K. Ueda, H. Hosono, *Appl. Phys. Lett.*, 2001, 78, 1583. <sup>6</sup> N. Duan, A. W. Sleight, M. K. Jayaraj, and J. Tate, *Appl. Phys. Lett.*, 2000 77, 1325.
- H. Kawazoe, H. Yanagi, K. Ueda, and H. Hosono, *MRS Bull.*, 2000, 25, 28.
- R. Nagarajan, N. Duan, M. K. Jayaraj, J. Li, K. A. Vanaja, A. Yokochi, A. Draeseke, J. Tate, and A. W. Sleight, *Int. J. Inorg. Mater.*, 2001, 3, 265–270.
- M. Snure and A. Tiwari, *Appl. Phys. Lett.*, 2007, 91, 092123.
- F. A. Benko and F. P. Koffyberg, *Mater. Res. Bull.*, 1986, 21, 753–757.
- C. Rastogi, S. H. Lim, and S. B. Desu, *J. Appl. Phys.*, 2008, 104, 032712.
- D. Li, X. D. Fang, Z. H. Deng, S. Zhou, R. H. Tao, W. W. Dong, T. Wang, Y. P. Zhao, G. Meng, and X. B. Zhu, *J. Phys. D: Appl. Phys.*, 2007, 40, 4910–4915.
- D. O. Scanlon and G. W. Watson, *J. Mater. Chem.*, 2011, 21, 3655.
- R. Bywalez, S. Gotzendorfer, and P. Lobmann, *J. Mater. Chem.*, 2010, 20, 6562–6570.
- Y. Ma, X. Zhou, Q. Ma, A. Litke, P. Liu, Y. Zhang, C. Li, and E. J. M. Hensen, *Catal Lett*, 2014, 144, 1487–1493.
- S. Zhou, X. Fang, Z. Deng, D. Li, W. Dong, and R. Tao, *Sensors and Actuators B*, 2009, 143, 119.
- Y. Ono, K. Satoh, T. Nozaki, and T. Kajitani, *Jpn. J. Appl. Phys.*, 2007 46, 1071–1075.
- T. Okuda, N. Jufuku, S. Hidaka, and N. Terada, *Phys. Rev. B*, 2005, 72, 144403.
- K. Hayashi, K. Sato, T. Nozaki, and T. Kajitani, *Jpn. J. Appl. Phys.*, 2008, 47, 59–63.
- G. B. Dong, M. Zhang, X. P. Zhao, H. Yan, C. Y. Tian, and Y. G. Ren, *Appl. Surf. Sci.*, 2010, 256, 4121-4124.
- X. S. Zhou, F. T. Lin, W. Z. Shi, A. Y. Liu, *J. Alloys Compd.*, 2014, 614, 221-225.